The Formation of Silylated β-Lactams from Silylketenes through Lewis Acid Promoted [2+2] Cycloaddition: A Combined Theoretical and Experimental Study

Béatrice Pelotier,[a] Michel Rajzmann,[a] Jean-Marc Pons,[a] Pablo Campomanes,[b] Ramón López,[b] and Tomás L. Sordo*[b]

Keywords: Silylketenes / Lactams / Lewis acids / Reaction mechanisms / Density functional calculations

The stereoselective formation of silylated *cis*-β-lactams from (trimethylsilyl)ketene and an α-imino ester by Lewis acid catalysis is described. Theoretical results suggest that the reaction between (trimethylsilyl)ketene and *trans*-(methoxycarbonyl)-*N*-methylformaldimine would proceed most favourably with the BF_3 catalyst coordinated to the ketene. Moreover, the calculated energy barriers account for the *cis*:*trans* ratio found experimentally.

Introduction

The Staudinger [2+2] cycloaddition reaction between an imine and a ketene has been known for nearly a century[1] and is still widely used to prepare β-lactams.[2] The mechanism of the reaction involves stereoselective attack by the lone pair of the nitrogen atom of the imine on the central carbon atom of the ketene and subsequent conrotatory electrocyclisation of the resultant zwitterionic intermediate to give the *cis*-β-lactam (Scheme 1). The mechanism is based both on experimental evidence of the occurrence of a zwitterionic intermediate[3] and on theoretical studies.[4]

Examples of the use of silylketenes[5] in β-lactam synthesis are rather scarce and always involve an electron-poor imine.[6,7] A typical example is provided by Zaitsevaand co-workers[7] who prepared a *trans*-silylated β-lactam from (trimethylsilyl)ketene (**1**)[8] and (methylsulfonyl)chloraldimine (see Scheme 2).[7] No Lewis acid was used in any of these examples.

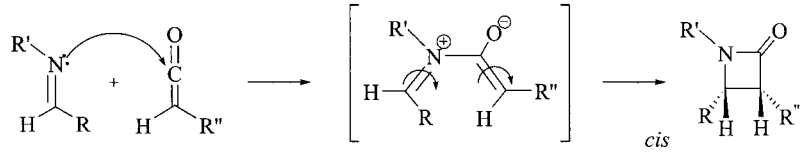

Scheme 1.

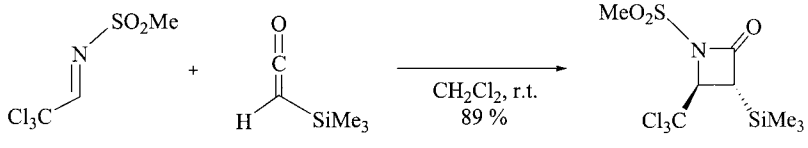

Scheme 2.

Our experience of silylketene chemistry led us to propose that these compounds could in certain circumstances behave as nucleophiles, for example, in the Lewis acid catalysed formation of β-lactones from aldehydes. This conclusion, based on experimental[9] and theoretical work,[10] and the above-mentioned reactivity of silylketenes

[a] Laboratoire SYMBIO (UMR CNRS 6178), Equipe RéSO, Université Paul Cézanne, Faculté des Sciences et Techniques, Service D12, 13397 Marseille Cedex 20, France
E-mail: jean-marc.pons@univ.u-3mrs.fr
[b] Departamento de Química Física y Analítica, Universidad de Oviedo,
Julián Clavería 8, 33006, Oviedo, Principado de Asturias, Spain
E-mail: tsordo@uniovi.es
Supporting information for this article is available on the WWW under http://www.eurjic.com or from the author.

towards imines[6,7] led us to study, both experimentally and theoretically, the formation of β-lactams from silylketenes and imines under Lewis acid catalysis conditions. The publication of a study of a catalysed Staudinger reaction[11] prompted us to publish our results.[12]

Results and Discussion

Experimental Study

The study was carried out with two different imines: a standard one, *n*-hexanaldimine **2**, and an electron-poor one, *n*-butyl glyoxylate imine **3** (see Scheme 3). The latter was chosen since it is a fairly stable compound that can be stored and because it gives reproducible results.[13] (trimethylsilyl)ketene (**1**) and BF_3–Et_2O were the other reagents used in the reaction which was carried out in Et_2O.

It appears from Scheme 3 that the desired reaction occurs only when the glyoxylate imine **3** and BF_3–Et_2O react with (trimethylsilyl)ketene **1**. Indeed, β-lactam **4** is formed in fair yield as a 60:15:15:10 (*cis*:*cis*:*trans*:*trans*) mixture of four diastereoisomers (determined by 400 MHz ^1H NMR spectroscopy). In the other three cases, at temperatures at or below 0 °C only the starting materials were recovered. When the temperature was allowed to rise to room temperature, a complex mixture of products was formed (resulting from the degradation of the starting materials) but no β-lactams (silylated or not) were observed.

The yields of β-lactam **4** were disappointing when various other Lewis acids were used ($SnCl_4$: 0%; $AlCl_3$: 20%; $EtAlCl_2$ and TMSOTf: 35% yields). With $MgBr_2$–Et_2O, the β-lactam ring was formed in 84% yield but it was not possible to prevent desilylation: β-lactam **4** was obtained along with the corresponding desilylated molecule (up to 50% of the reaction yield). With BF_3–OEt_2 as the Lewis acid, the use of other solvents did not lead to better yields of β-lactam **4** (CH_2Cl_2: 30%; toluene: 39%) and had very little effect on the *cis*:*trans* ratio (CH_2Cl_2: 78:22; toluene: 74:26).

In order to improve our understanding of the mechanism of this reaction, we also performed low-temperature ^{13}C NMR experiments (100.3 MHz, $CDCl_3$); the main observations are as follows:

i) No complexation between silylketene **1** and BF_3–Et_2O can be observed between –40 and 20 °C (i.e. no shift in the signals corresponding to silylketene **1** and complexed-Et_2O carbon atoms occurred).

ii) Imine **3**–BF_3 complexes can be observed at –40 °C (see Expt. Sect.).

iii) β-Lactam **4** is formed in the NMR tube at –40 °C.

Since no intermediate, except the imine–BF_3 complex, was observed directly, we decided to investigate the mechanism of the reaction by theoretical means.

Theoretical Study

It is well known that the Staudinger reaction between ketenes and imines involves low energy barriers allowing the quick formation of β-lactams even at reduced temperatures.[14] However, the presence of a silyl substituent on the ketene slows the process considerably and therefore, in general, a catalyst is required. Indeed, our calculations of the Staudinger reaction at the B3LYP/6-311+G(d,p)/PCM//B3LYP/6-311+G(d,p) level of theory reveal that the rate-determining barrier for the uncatalysed reaction between methylketene and formaldimine, which corresponds to the electrocyclic conrotatory closure of the zwitterionic intermediate, has a value of 17.1 kcal mol^{-1} for the *anti* approach and 23.2 kcal mol^{-1} for the *syn* approach, whereas for the reaction with silylketene, the corresponding values are 26.2 and 25.2 kcal mol^{-1}, respectively (see Figure 1). These calculations are in agreement with the fact that silylketenes are much more stable than alkylketenes.

In order to investigate the mechanism of the Staudinger reactions studied experimentally, we calculated the energy profiles for the reactions of silylketene ($H_3SiCH=C=O$) with *trans*-(methoxycarbonyl)-*N*-methylformaldimine (R^2 = CO_2Me) and *trans*-*N*-methyl-methylformaldimine (R^2 = Me) catalyzed by BF_3 as Lewis acid. These two imines were chosen as models for imines **3** and **2**, respectively, while silylketene was used as a model for (trimethylsilyl)ketene (**1**).

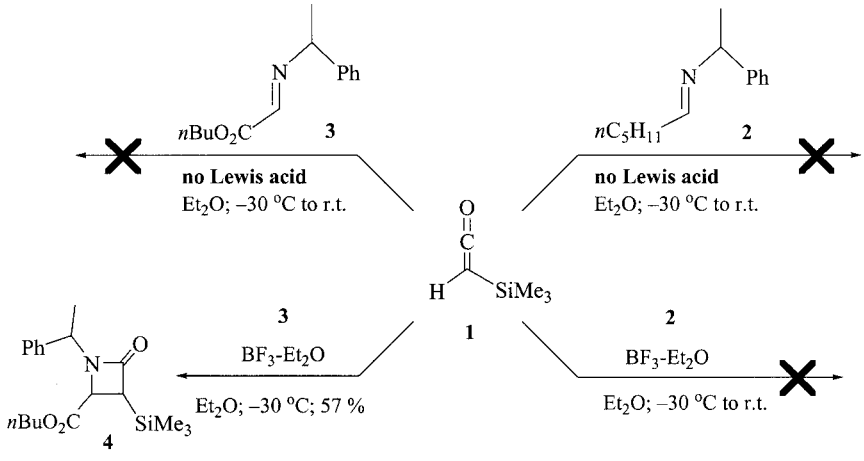

Scheme 3.

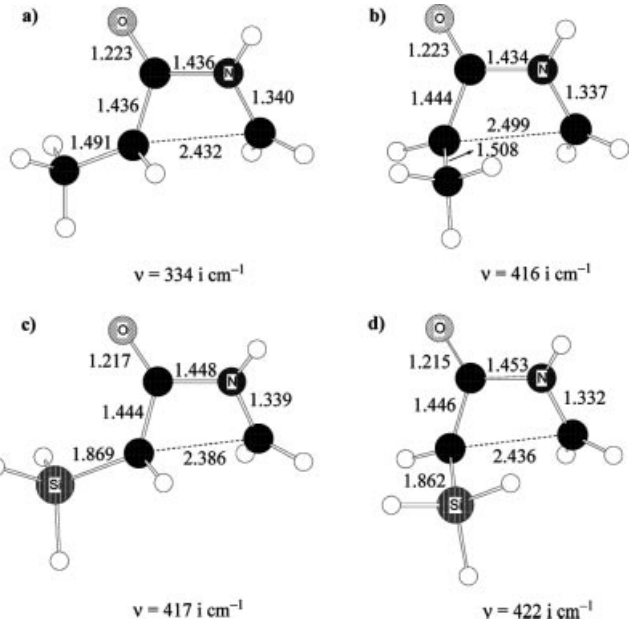

Figure 1. B3LYP/6-311+G(d,p)-optimized geometries of the transition states for the electrocyclic conrotatory closure step for the reactions between methylketene and formaldimine by a) the *anti* and b) the *syn* approaches, and between silylketene and formaldimine by c) the *anti* and d) the *syn* approaches. Lengths are given in Ångstrøms.

The catalyst may bond to the nitrogen atom of the imine and induce a reverse electron demand mechanism or to the oxygen atom of the ketene and induce a catalyzed Staudinger mechanism (see Scheme 4).

Reaction between Silylketene and *trans*-(Methoxycarbonyl)-*N*-methylformaldimine in the Presence of BF_3

The energies of all the critical structures of both the reverse electron demand and the catalyzed Staudinger mechanisms are given in Table 1 and Figure 2 shows the corresponding energy profiles in solution. The B3LYP/6-311+G(d,p)/PCM//B3LYP/6-311+G(d,p)/Onsager energies, including the zero-point vibrational energy (ZPVE) correction from the Onsager frequencies, are given in the text.

Reverse Electron Demand Mechanism

Figure 1S (available in the Supporting Information; see also the footnote on the first page of this article), shows the optimized geometries of the critical structures located in the reverse electron demand mechanism.

The BF_3 catalyst coordinated to the imine gives rise to a complex, **C1*cN***, that is 17.8 kcal mol^{-1} more stable than the reactants. This complex has been experimentally detected (vide supra). **C1*cN*** and the ketene can react by three different routes: when the two reactants approach with the silyl and methoxycarbonyl substituents in a *trans* arrangement, both concerted and stepwise mechanisms are possible whereas the corresponding *cis* interaction only gives rise to a stepwise path. **C1*cN*** reacts by the *trans* concerted route through transition state **TS3*cN*$_{trans}$**, which is 8.9 kcal mol^{-1} above the reactants giving an energy barrier of 26.7 kcal mol^{-1}, to yield the corresponding β-lactam with BF_3 coordinated to the nitrogen atom, **C2*cN*$_{trans}$**, 16.3 kcal mol^{-1} below the energy of the reactants. By the

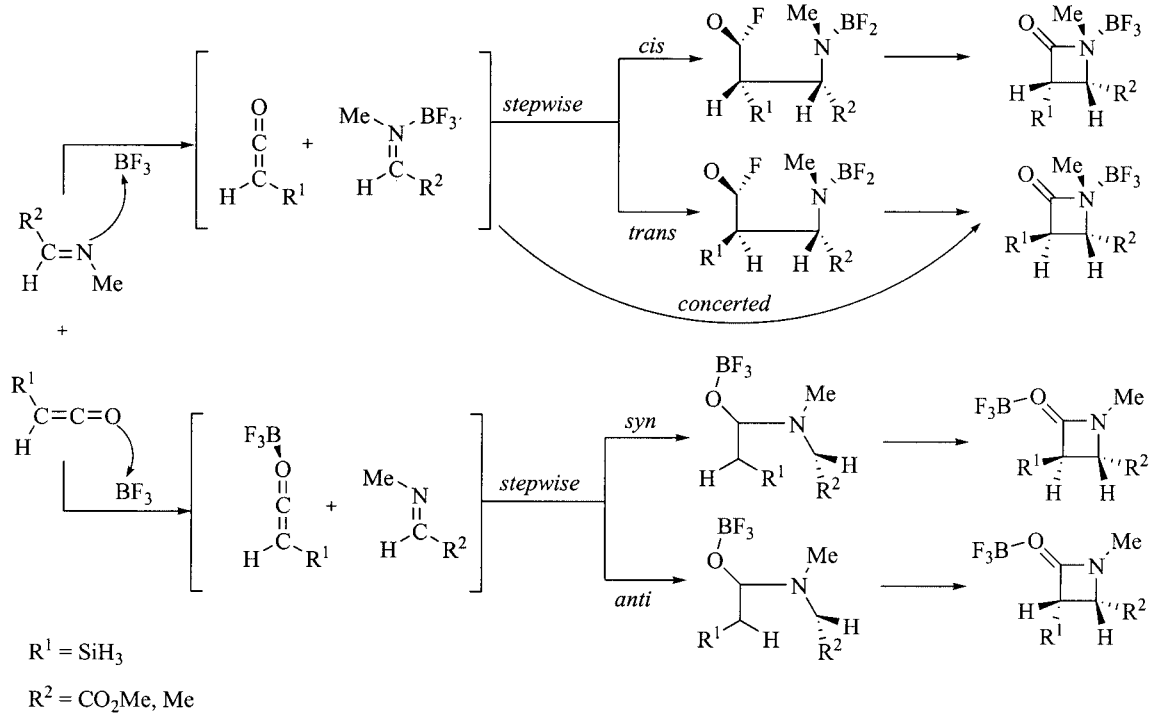

Scheme 4.

Table 1. Relative B3LYP/6-311+G(d,p) electronic energies in the gas phase (including ZPVE) (ΔE) and relative B3LYP/6-311+G(d,p)/PCM//B3LYP/6-311+G(d,p)/Onsager energies (including ZPVE corrections from Onsager frequency calculations) ($\Delta E_{solution}$) of the structures located for the reaction of silylketene with *trans*-(methoxycarbonyl)-*N*-methylformaldimine with (top) and without (bottom) the BF_3 catalyst.

Structures	ΔE/kcal mol^{-1}	$\Delta E_{solution}$/kcal mol^{-1}
BF_3 + ketene + imine	0.0	0.0
C1*cN* + ketene	–14.0	–17.8
TS1*cN*$_{trans}$	9.1	7.5
I*cN*$_{trans}$	–18.2	–14.1
TS2*cN*$_{trans}$	7.6	8.4
TS1*cN*$_{cis}$	14.9	11.1
I*cN*$_{cis}$	–12.2	–9.4
TS2*cN*$_{cis}$	10.4	10.4
TS3*cN*$_{trans}$	14.1	8.9
C2*cN*$_{cis}$	–17.5	–18.1
C2*cN*$_{trans}$	–37.8	–16.3
C1*cO* + imine	–1.9	–0.5
TS1*cO*$_{anti}$	4.9	7.6
I*cO*$_{anti}$	–1.1	–3.5
TS2*cO*$_{anti}$	13.4	8.7
TS1*cO*$_{syn}$	7.2	9.3
I*cO*$_{syn}$	4.2	–3.6
TS2*cO*$_{syn}$	13.5	9.1
C2*cO*$_{trans}$	–31.0	–34.3
C2*cO*$_{cis}$	–29.6	–32.7
Ketene + imine	0.0	0.0
TS2$_{syn}$	28.5	28.0
TS2$_{anti}$	27.3	27.1
trans-β-Lactam	–18.9	–17.8
cis-β-Lactam	–17.5	–16.0

trans stepwise path, **C1*cN*** reacts via transition state **TS1*cN*$_{trans}$**, 7.5 kcal mol^{-1} above the reactants, to form an intermediate, **I*cN*$_{trans}$**, that is 21.6 kcal mol^{-1} more stable. Intermediate **I*cN*$_{trans}$** then yields the β-lactam–BF_3 complex, **C2*cN*$_{trans}$**, via the transition state **TS2*cN*$_{trans}$**, which is 8.4 kcal mol^{-1} less stable than the reactants. Hence, the first step is rate-determining with an activation barrier of 25.3 kcal mol^{-1}. When the reactants approach with the silyl and methoxycarbonyl substituents in the *cis* orientation, the reaction between **C1*cN*** and the silylketene evolves along a two-step mechanism analogous to the previous one via transition state **TS1*cN*$_{cis}$**, intermediate **I*cN*$_{cis}$** and transition state **TS2*cN*$_{cis}$** (with relative energies with respect to the reactants of 11.1, –9.4, and 10.4 kcal mol^{-1}, respectively) to afford the *cis*-β-lactam–BF_3 complex which is 18.1 kcal mol^{-1} more stable than the reactants. Therefore, the first stage of this mechanism is rate-determining with an energy barrier of 28.9 kcal mol^{-1}.

Catalyzed Staudinger Mechanism

Figure 3 shows the optimized geometries of the critical structures located in the Staudinger mechanism.

When the catalyst is coordinated to silylketene, complex **C1*cO*** is formed which is 0.5 kcal mol^{-1} more stable than the reactants. When the imine approaches **C1*cO*** in an *anti* orientation with respect to the silyl substituent a two-step mechanism results involving transition state **TS1*cO*$_{anti}$**, intermediate **I*cO*$_{anti}$** and transition state **TS2*cO*$_{anti}$** with relative energies of 7.6, –3.5 and 8.7 kcal mol^{-1}, respectively, to yield the *cis*-β-lactam–BF_3 complex, **C2*cO*$_{cis}$**, 32.7 kcal mol^{-1} lower than the reactants.

Thus, the second step is rate-determining with an energy barrier of 12.2 kcal mol^{-1}. When **C1*cO*** approaches the imine with a *syn* orientation, the system evolves along an analogous two-step route through transition state **TS1*cO*$_{syn}$** (9.3 kcal mol^{-1}), intermediate **I*cO*$_{syn}$** (–3.6 kcal mol^{-1}) and transition state **TS2*cO*$_{syn}$** (9.1 kcal mol^{-1}) to give the *trans*-β-lactam–BF_3 complex, **C2*cO*$_{trans}$**, that is 34.3 kcal mol^{-1}

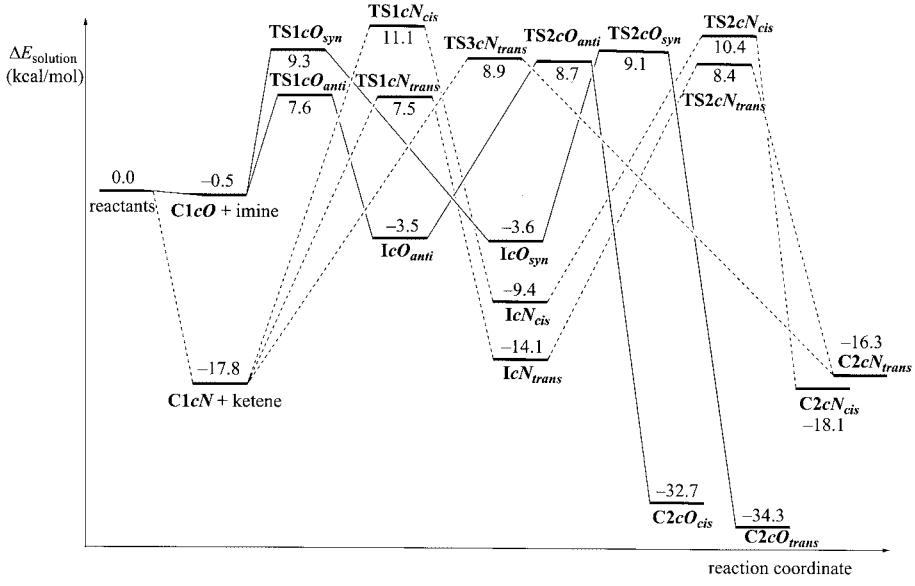

Figure 2. B3LYP/6-311+G(d,p)/PCM//B3LYP/6-311+G(d,p)/Onsager+ZPVE(B3LYP/Onsager) energy profiles for the reaction between silylketene and *trans*-(methoxycarbonyl)-*N*-methylformaldimine in the presence of BF_3.

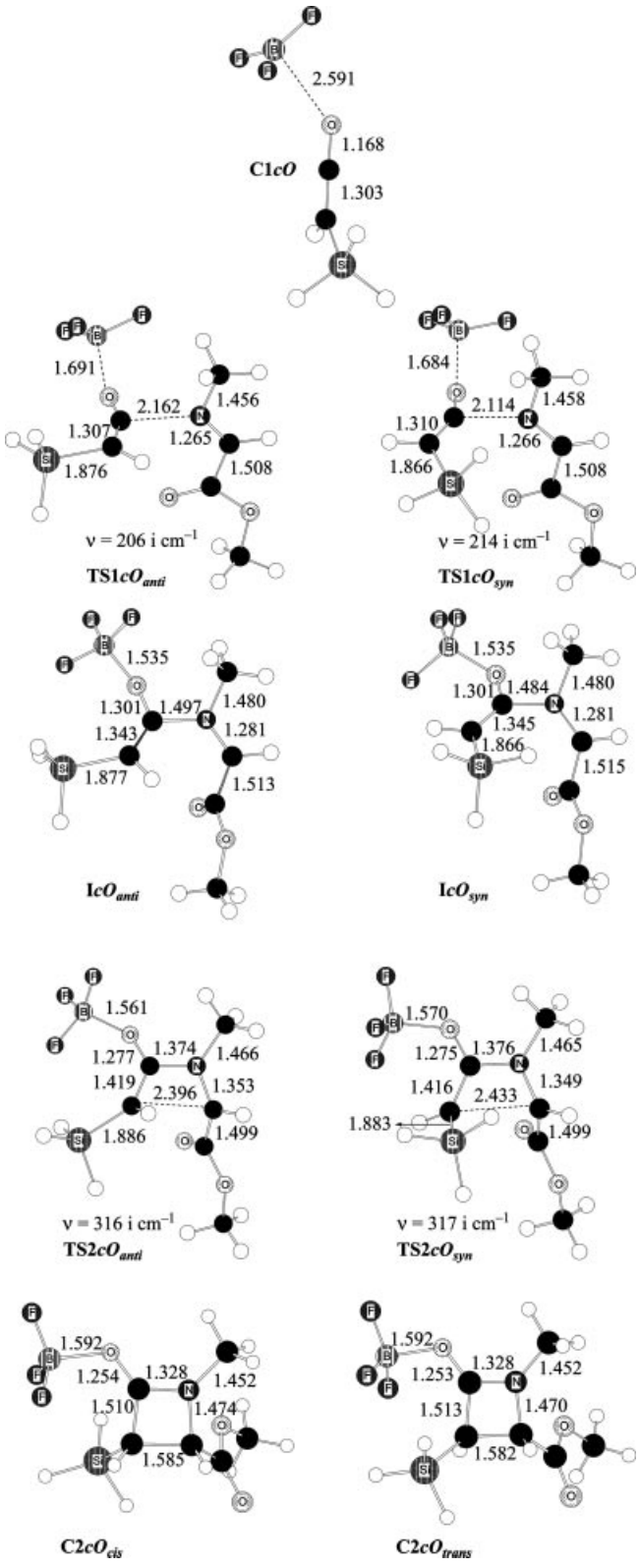

Figure 3. B3LYP/6-311+G(d,p)/Onsager optimized geometries of the critical structures for the catalyzed Staudinger mechanism for the reaction between silylketene and *trans*-(methoxycarbonyl)-*N*-methylformaldimine in the presence of BF_3. Lengths are given in Ångstrøms.

more stable than the original reactants. Here again the second stage of the reaction is rate-determining with an energy barrier of 12.7 kcal mol^{-1}.

Discussion and Comparison with Experiment

It is clear from these calculations that the catalyzed Staudinger mechanism is the favoured one and hence the following rationalization of the experimental results can be proposed. Initially roughly half the ketene and imine are complexed to BF_3 leading to the imine–BF_3 and ketene–BF_3 complexes. On one hand, given its relative thermodynamic stability, the BF_3–imine complex is involved in no (or very little) cycloaddition resulting in a yield of β-lactam of about 50%, in good agreement with the experimental results obtained for the reaction between silylketene **1** and glyoxylate imine **3** (see Scheme 3). On the other hand, despite its low relative stability, most of the cycloaddition reaction occurs from the ketene–BF_3 complex because of the low activation barriers in the routes starting from this point. These relatively low activation barriers result from a stronger complexation of BF_3 to the oxygen atom of the ketene in the transition state structures (1.691 or 1.684 Å) than in the initial ketene–BF_3 complex (2.591 Å). The difference in the rate-determining energy barrier between the *syn* (12.7 kcal mol^{-1}) and *anti* (12.2 kcal mol^{-1}) approaches of the **C1*cO*** and imine renders a theoretical *cis*:*trans* ratio for the β-lactam–BF_3 complex at –30 °C of 74:26, close to the experimental value. Note that the asymmetric induction experimentally observed, particularly in the case of the *cis* isomers (see Scheme 3), can be attributed to the fact that the difference between the two faces of the β-lactam ring introduced by the chiral substituent on the nitrogen atom of the imine employed in the experimental work has a larger effect on the two *cis* isomers because in the corresponding rate-determining transition states the two substituents appear on the same face whereas in the transition states for the *trans*-β-lactams there is a substituent on each face.

Note that the β-lactam–BF_3 complexes in which the catalyst is coordinated to the nitrogen atom are considerably less stable than those in which BF_3 is coordinated to the oxygen atom. This is clearly a consequence of the hindrance of the conjugation between the lone pair on the nitrogen atom and the C–O double bond in the β-lactam ring, which is also reflected in a lengthening of the C–N bond length of about 0.15 Å compared with the length of the C–N bond in the isolated β-lactam ring (approximately 1.37 Å).

The catalytic effect of BF_3 in these processes is very important. As shown at the bottom of Table 1 the rate-determining energy barriers for the formation of the *cis*- and *trans*-β-lactams in solution without the Lewis acid catalyst are 27.1 and 28.0 kcal mol^{-1}, respectively, more than double the values for the most favourable catalyzed mechanisms.

Note also that in the presence of BF_3 as catalyst, the energy barriers for the most favourable mechanisms of the reaction between silylketene and *trans*-*N*-methyl-methylformaldimine (R^2 = Me) are relatively high, in agreement with

the experimental observation that no reaction between the silylketene **1** and *n*-hexanaldimine **2** occurs even with the aid of a catalyst. Indeed, from Table 2 we can see that the rate-determining energy barriers in solution for the *anti* and *syn* mechanisms are 26.6 and 26.3 kcal mol^{-1}, respectively.

Table 2. Relative B3LYP/6-311+G(d,p) electronic energies in the gas phase (including ZPVE) (ΔE) and relative B3LYP/6-311+G(d,p)/PCM//B3LYP/6-311+G(d,p)/Onsager energies (including ZPVE corrections from Onsager frequency calculations) ($\Delta E_{solution}$) of the most significant structures located for the reaction of silylketene with *trans*-*N*-methyl-methylformaldimine in the presence of BF_3.

Structures	ΔE/kcal mol^{-1}	$\Delta E_{solution}$/kcal mol^{-1}
BF_3 + ketene + imine	0.0	0.0
C1*cO* + imine	–1.9	–0.5
TS1cO_{anti}	1.8	4.9
IcO_{anti}	–10.8	–18.8
TS2cO_{anti}	17.4	7.8
TS1cO_{syn}	3.9	6.0
IcO_{syn}	–5.7	–20.2
TS2cO_{syn}	16.4	6.1

Figure 2S, available in the Supporting Information, shows the corresponding critical structures. Our theoretical results clearly indicate that the increase in the rate-determining energy barrier that arises when an electron-rich imine is employed does not stem from a destabilisation of the corresponding transition state with respect to the reactants, but from an important stabilisation of the intermediate preceding this transition state that results from the presence of the methyl substituent on the carbon atom of the imine.

Conclusions

A catalyzed Staudinger mechanism accounts for both the overall yield and the diastereoselectivity of the [2+2] cycloaddition reaction of silylketenes with imines leading to β-lactams. Despite the fact that reaction paths corresponding to the reverse electron demand mechanism were found, they cannot account for the occurrence of the reaction at low temperature, mainly because of the high stability of the imine–BF_3 complex, or for its diastereoselectivity.

Experimental Section

All reactions were magnetically stirred and were monitored by thin-layer chromatography (TLC) using Macherey–Nagel Düren Alugram Si G/UV_{254} pre-coated aluminium foil sheets, layer thickness 0.25 mm. Compounds were visualised by UV (254 nm) detection and then with 20 wt-% phosphomolybdic acid (PMA) in ethanol with heating. Organic extracts were dried with $MgSO_4$ unless otherwise specified and solvents were evaporated at a water pump using a Buchi rotary evaporator. Petroleum ether (boiling range 40–60 °C) and diethyl ether ("ether") were used as eluents in chromatography and were distilled before use. Column chromatography was performed using Merck silica gel 60 (0.04–0.063 mm, 230–400mesh) under low pressure. When appropriate, solvents and reagents were dried by distillation from the usual drying agent prior to use. Diethyl ether was distilled from Na/benzophenone and used fresh. Dichloromethane was distilled from P_2O_5. IR spectra were recorded with a Perkin–Elmer 1600 series FTIR spectrometer as thin films supported on sodium chloride plates. Absorptions are reported in cm^{-1} and defined as either strong (s), medium (m) or weak (w). ^{1}H NMR spectra were recorded in Fourier transform mode with a Bruker AC 200 (200 MHz) or AM 400 (400 MHz) spectrometer in [D]chloroform. Chemical shifts are reported in ppm relative to residual $CHCl_3$ (δ = 7.27 ppm). Multiplicities are described using the following abbreviations: (s) singlet, (d) doublet, (t) triplet, (q) quartet, (quint) quintet, (sext) sextet, (sept) septuplet, (m) multiplet and (br) broad. ^{13}C NMR spectra were recorded with a Bruker AC 200 (50.3 MHz) or AC 400 (100.6 MHz) spectrometer in [D]chloroform. Chemical shifts are reported in ppm relative to the solvent (δ = 77.1 ppm). Multiplicities were determined by using the distortionless enhancement by polarization transfer (DEPT) spectral editing technique. The number of coupled protons is indicated by an integer 0–3 in parentheses following the ^{13}C chemical shift value. Mass spectra were recorded on a VO 70–250-SE or JEOL MStation JMS-700 spectrometer. Ion mass/charge (*m*/*z*) ratios are reported as atomic mass units followed, in parentheses, by the peak intensity relative to the base peak (100%) and where shown, the proposed signal assignment. All compounds submitted for mass spectral analysis were purified by either distillation or column chromatography and estimated to be at least 95% pure by NMR and thin-layer chromatography.

(Trimethylsilyl)ketene (1):[8]

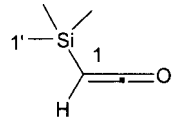

2-Ethoxy-1-(trimethylsilyl)acetylene (3.45 g, 24.2 mmol) was quickly introduced into a flask fitted with a short-path distillation apparatus pre-warmed to 130–135 °C in an oil bath. The pyrolysis was followed by the bubbling of gaseous ethylene formed in situ. Pure (trimethylsilyl)ketene (**1**) (b.p. 80–82 °C) was obtained as a colourless oil after distillation (1.71 g, 15.0 mmol, 62%). IR (film): $\tilde{\nu}$ = 2110 (s), 1270 (m), 1250 (m), 1055 (w), 845 (s), 755 (w) cm^{-1}. ^{1}H NMR (200 MHz, $CDCl_3$): δ = 1.81 (s, 1 H), 0.19 (s, 9 H) ppm. ^{13}C NMR (50.3 MHz, $CDCl_3$): δ = 179.5 (0), 0.6 (3, 3C), –0.2 (1) ppm.

***N*-(1′-Phenylethyl)hexanaldimine (2):**[15]

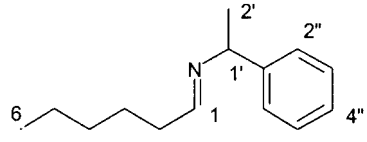

A solution of freshly distilled hexanal (551 mg, 5.5 mmol) in CH_2Cl_2 (15 mL) was introduced, under argon, into a flask containing 3-Å molecular sieves (1 g). 1-(Phenyl)ethylamine (645 µL, 5 mmol) was then added dropwise and the mixture was stirred at room temperature for 30 min. The molecular sieves were then filtered off and the solvent evaporated in vacuo to give crude imine **2** as a colourless oil which was used directly in the [2+2] cycloaddition reaction. IR (film): $\tilde{\nu}$ = 1670 (s), 1490 (m), 1380 (m), 760

(m), 700 (s) cm^{-1}. ^1H NMR (200 MHz, $CDCl_3$): δ = 7.75 (t, J = 5.1 Hz, 1 H, H-1), 7.40–7.20 (m, 5 H, H-2′′. H-3′′, H-4′′), 4.28 (q, J = 6.6 Hz, 1 H, H-1′), 2.28 (td, J = 7.2, 5.1 Hz, 2 H, H-2), 1.50 (d, J = 6.6 Hz, 3 H, H-2′), 1.40–1.20 (m, 6 H, H-3, H-4, H-5), 0.89 (t, J = 6.4 Hz, 3 H, H-6) ppm. ^{13}C NMR (50.3 MHz, $CDCl_3$): δ = 163.6 (1), 144.9 (0), 128.1 (1, 2C), 126.7 (1), 126.3 (1, 2C), 69.5 (1), 35.6 (2), 31.3 (2), 25.6 (2), 24.4 (3), 22.2 (2), 13.8 (3) ppm.

Butyl-*N*-(1′-phenylethyl)glyoxaldimine (3):[13]

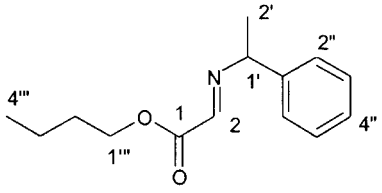

A solution of freshly prepared butyl glyoxylate (252 mg, 1.94 mmol) in CH_2Cl_2 (5 mL) was introduced, under argon, into a flask containing 3 Å molecular sieves (400 mg). 1-(Phenyl)ethylamine (263 μL, 2.04 mmol) was then added dropwise and the mixture was stirred at room temperature for 30 min. The molecular sieves were then filtered off and the solvent evaporated in vacuo to give the crude imine. Purification by flash chromatography (petroleum ether/ether, 4:1) led to pure imine **3** (426 mg, 1.83 mmol) in 94% yield. IR (film): $\tilde{\nu}$ = 1720 (s), 1650 (w), 1290 (m), 1195 (s), 735 (m), 700 (s) cm^{-1}. ^1H NMR (200 MHz, $CDCl_3$): δ = 7.74 (s, 1 H, H-2), 7.42–7.20 (m, 5 H, H-2′′. H-3′′, H-4′′), 4.61 (q, J = 6.6 Hz, 1 H, H-1′), 4.28 (t, J = 7.2 Hz, 2 H, H-1′′′), 1.69 (quint, J = 7.2 Hz, 2 H, H-2′′′), 1.63 (d, J = 6.6 Hz, 3 H, H-2′), 1.41 (sext, J = 7.2 Hz, 2 H, H-3′′′), 0.95 (t, J = 7.2 Hz, 3 H, H-4′′′) ppm. ^{13}C NMR (50.3 MHz, $CDCl_3$): δ = 163.2 (0), 152.2 (1), 142.7 (0), 128.6 (1, 2C), 127.4 (1), 126.8 (1, 2C), 69.6 (1), 65.5 (2), 30.5 (2), 23.8 (3), 19.0 (2), 13.6 (3) ppm.

3–BF_3 Complexes:[16] The most significant changes in the ^{13}C NMR (50.3 MHz, $CDCl_3$) spectrum of **3** upon complexation of BF_3 are as follows: Signals that have shifted: 163.2, 152.2, 142.7, 69.6 ppm; new signals:[16] 161.5, 159.7, 157.5, 137.2, 136.2, 135.9, 67.9 ppm.

4-(Butoxycarbonyl)-*N*-(1′-phenylethyl)-3-(trimethylsilyl)-2-azetidinone (4):

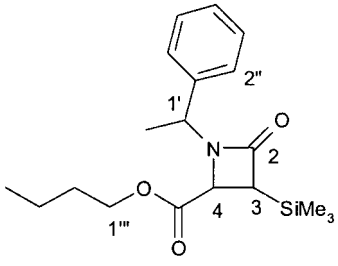

To a mixture of imine **3** (117 mg, 0.5 mmol) and (trimethylsilyl) ketene (**1**) (68 mg, 0.6 mmol) in Et_2O (2 mL) at –50 °C was added BF_3–Et_2O (68 μL, 0.55 mmol). The reaction was stirred for 2 h between –50 and –30 °C before hydrolysis (2 mL H_2O). After extraction with Et_2O (3 × 3 mL), the organic layer was washed with brine and dried with $MgSO_4$. Evaporation of the solvent in vacuo led to the crude product which was purified by chromatography (petroleum ether/ether, 4:1) to yield 2-azetidinones **4** (99 mg, 0.28 mmol, 57%) as a colourless oil as a 60:15:15:10 (*cis*/*cis*/*trans*/*trans*) mixture of four diastereoisomers. Note: This diastereomeric ratio is based on the integrals of the peaks corresponding to protons H-3 and H-4 of the four diastereoisomers.

IR (film): $\tilde{\nu}$ = 1750 (s), 1250 (s), 1185 (s), 1095 (m), 1030 (m), 850 (s), 700 (m) cm^{-1}. Major *cis* isomer: ^1H NMR (400 MHz, $CDCl_3$): δ = 7.36–7.28 (m, 5 H, H-2′′. H-3′′, H-4′′), 4.99 (q, J = 7.1 Hz, 1 H, H-1′), 4.17–3.95 (m, AB syst, 2 H, H-1′′′), 3.91 (d, J = 6.0 Hz, 1 H, H-4), 2.91 (d, J = 6.1 Hz, 1 H, H-3), 1.62 (d, J = 6.9 Hz, 3 H, H-2′), 1.60 (m, 2 H, H-2′′′), 1.34 (sext, J = 7.4 Hz, 2 H, H-3′′′), 0.93 (t, J = 7.3 Hz, 3 H, H-4′′′), 0.12 (s, 9 H, H-1′′′′) ppm. ^{13}C NMR (100.6 MHz, $CDCl_3$): δ = 171.2 (0), 169.0 (0), 139.6 (0), 128.6 (1, 2C), 127.7 (1), 127.6 (1, 2C), 65.2 (2), 52.6 (1), 52.1 (1), 45.8 (1), 30.4 (2), 19.1 (2), 18.8 (3), 13.6 (3), –2.0 (3, 3C) ppm. Minor *cis* isomer (distinct signals): ^1H NMR (400 MHz, $CDCl_3$): δ = 4.65 or 4.57 (q, J = 7.1 Hz, 1 H, H-1′), 2.97 (d, J = 6.3 Hz, 1 H, H-3), 1.79 or 1.75 (d, J = 7.0 Hz, 3 H, H-2′) ppm. Major *trans* isomer (distinct signals): ^1H NMR (400 MHz, $CDCl_3$): δ = 4.65 or 4.57 (q, J = 7.1 Hz, 1 H, H-1′), 3.64 (d, J = 2.8 Hz, 1 H, H-4), 2.67 (d, J = 2.7 Hz, 1 H, H-3), 1.79 or 1.75 (d, J = 7.0 Hz, 3 H, H-2′) ppm. Minor *trans* isomer (distinct signals): ^1H NMR (400 MHz, $CDCl_3$): δ = 3.58 (d, J = 2.5 Hz, 1 H, H-4), 2.69 (d, J = 2.5 Hz, 1 H, H-3) ppm. LRMS (CI mode): *m*/*z* (%) = 348.2 (100) $[M + H]^+$, 234.2 (15). HRMS (CI mode): found $[M + H]^+$ 348.1994; $C_{19}H_{29}NO_3Si$ + H requires 348.1995.

Computational Details: Quantum chemical computations were performed using the Gaussian 98 series of programs[17] with the hybrid density functional B3LYP.[18] The geometry of the critical structures located along the reaction coordinates were fully optimized using the 6-311+G(d,p) basis set[19] and Schlegel's algorithm.[20] Harmonic vibrational frequencies were also calculated at this same level of theory to characterize the critical points located and to evaluate the zero-point vibrational energy (ZPVE).

In the preliminary evaluation of the rate-determining energy barriers for the reactions of methylketene and silylketene with formaldimine we carried out single-point polarisable continuum model (PCM)[21] calculations on the gas-phase geometries. To take into account the effects of the condensed phase in the mechanisms of the reactions of silylketene with *trans*-(methoxycarbonyl)-*N*-methylformaldimine and *trans*-*N*-methyl-methylformaldimine we optimized the geometries in solution using the Onsager continuum model[22] and performed single point calculations on these geometries with the PCM.[21] A relative permittivity of 4.34 was used in the calculations to simulate ether as solvent. This methodology has previously proved to be adequate in the study of related cycloaddition reactions in solution.[23] The minima connected by each located transition state (TS) have been checked by intrinsic reaction coordinate (IRC) calculations[24] at the same level of theory.

Supporting Information: Figure 1S, B3LYP/6-311+G(d,p)/Onsager optimized geometries for the reverse electron demand mechanism for the reaction between silylketene and *trans*-(methoxycarbonyl)-*N*-methylformaldimine in the presence of BF_3. Figure 2S, most significant optimized structures located with the B3LYP/6-311+G(d,p)/Onsager level of theory for the catalyzed Staudinger mechanism of the reaction between silylketene and *trans*-*N*-methyl-methylformaldimine in the presence of BF_3.

Acknowledgments

We are grateful to Dr. L. Stella (CNRS, Marseille) and Prof. P. J. Kocienski (Leeds University, UK) for fruitful discussions, and to Dr. M. Oblin (Marseille) for preliminary semiempirical calcula-

tions. The Franco-British collaboration was supported by a RSC Journal grant to J.-M. P. P. C., R. L. and T. L. S. thank the Principado de Asturias for financial support (PB02–045).

[1] H. Staudinger, *Justus Liebigs Ann. Chem.* **1907**, *356*, 51.
[2] a) G. I. Georg, *The Organic Chemistry of β-Lactams*, VCH, New York, **1993**; b) C. Palomo, J. M. Aizpurua, I. Ganboa, M. Oiarbide, *Eur. J. Org. Chem.* **1999**, 3223–3235.
[3] a) J. Pacansky, J. S. Chang, D. W. Brown, W. Schwarz, *J. Org. Chem.* **1982**, *47*, 2233–2234; b) H. W. Moore, G. Hughes, K. Srinivasachar, M. Fernández, N. V. Nguyen, D. Schoon, A. Tranne, *J. Org. Chem.* **1985**, *50*, 4231–4238; c) J. E. Lynch, S. M. Riseman, W. L. Laswell, D. M. Tschaen, R. P. Volante, G. B. Smith, I. Shinkay, *J. Org. Chem.* **1989**, *54*, 3792–3796.
[4] a) J. A. Sordo, J. González, T. L. Sordo, *J. Am. Chem. Soc.* **1992**, *114*, 6249–6251; b) F. P. Cossío, J. M. Ugalde, X. López, B. Lecea, C. Palomo, *J. Am. Chem. Soc.* **1993**, *115*, 995–1004; c) F. P. Cossío, A. Arrieta, B. Lecea, J. M. Ugalde, *J. Am. Chem. Soc.* **1994**, *116*, 2085–2093; d) X. Assfeld, M. F. Ruiz-López, J. González, R. López, J. A. Sordo, T. L. Sordo, *J. Comput. Chem.* **1994**, *15*, 479–487; e) X. Assfeld, R. López, M. F. Ruiz-López, J. González, T. L. Sordo, J. A. Sordo, *J. Mol. Struct. (Theochem)* **1995**, *331*, 1–2; f) R. López, M. F. Ruiz-López, D. Rinaldi, J. A. Sordo, T. L. Sordo, *J. Phys. Chem.* **1996**, *100*, 10600–10608; g) D. C. Fang, X. Y. Fu, *Int. J. Quantum Chem.* **1996**, *57*, 1107–1114; h) A. Arrieta, B. Lecea, F. P. Cossío, *J. Org. Chem.* **1998**, *63*, 5869–5876; i) T. N. Truong, *J. Phys. Chem. B* **1998**, *102*, 7877–7881; j) P. V. Bharatam, R. S. Kumar, M. P. Mahajan, *Org. Lett.* **2000**, *2*, 2725–2728; k) A. Arrieta, F. P. Cossío, B. Lecea, *J. Org. Chem.* **2000**, *65*, 8458–8464; l) A. Venturini, J. González, *J. Org. Chem.* **2002**, *67*, 9089–9092; m) C. Zhou, D. M. Birney, *J. Am. Chem. Soc.* **2002**, *124*, 5231–5241.
[5] For reviews on silylketene chemistry, see: a) T. T. Tidwell, *Ketenes*, Wiley, New York, **1995**, pp. 348–368; b) A. Pommier, P. J. Kocienski, J.-M. Pons, *J. Chem. Soc., Perkin Trans. 1* **1998**, 2105–2118.
[6] a) W. T. Brady, R. A. Owens, *Tetrahedron Lett.* **1976**, *17*, 1553–1556; b) J. Kron, U. Schubert, *J. Organomet. Chem.* **1989**, *373*, 203–219.
[7] a) O. P. Novikova, L. I. Livantsova, G. S. Zaitseva, *Zh. Obshch. Khim.* **1989**, *59*, 2630–2631; b) G. S. Zaitseva, O. P. Novikova, L. I. Livanstova, V. S. Petrosyan, Y. I. Baukov, *Zh. Obshch. Khim.* **1991**, *61*, 1389–1395.
[8] a) L. L. Shchukovskaya, R. I. Pal'Chick, A. N. Lazarev, *Dokl. Akad. Nauk SSSR* **1965**, *164*, 357 (*Chem. Abstr.* **1965**, *63*, 18138g); b) J. L. Loebach, R. L. Danheiser *in Encyclopedia of Reagents for Organic Synthesis* (Ed.: L. A. Paquette), Wiley, New York, **1995**, p. 5266.
[9] a) A. Pommier, J.-M. Pons, P. J. Kocienski, L. Wong, *Synthesis* **1994**, 1294–1300; b) P. J. Kocienski, B. Pelotier, J.-M. Pons, H. Prideaux, *J. Chem. Soc., Perkin Trans. 1* **1998**, 1373–1382.
[10] J.-M. Pons, M. Oblin, A. Pommier, M. Rajzmann, D. Liotard, *J. Am. Chem. Soc.* **1997**, *119*, 3333–3338.
[11] H. Wack, W. J. Drury, A. E. Taggi, D. Ferraris, T. Lectka, *Org. Lett.* **1999**, *1*, 1985–1988.
[12] B. Pelotier, Ph. D. Thesis, Université Paul Cézanne, Marseille, **1999**.
[13] H. Abraham, L. Stella, *Tetrahedron* **1992**, *48*, 9707–9718.
[14] A. E. Taggi, A. M. Hafez, H. Wack, B. Young, D. Ferraris, T. Lectka, *J. Am. Chem. Soc.* **2002**, *124*, 6626–6635, and references therein.
[15] C. Boga, D. Savoia, A. Umani-Ronchi, *Tetrahedron: Asymmetry* **1990**, *1*, 291–294.
[16] Since imine **3** bears several electronic doublets, several Lewis base–Lewis acid type complexes may be formed.
[17] M. J. Frisch, G. W. Trucks, H. B. Schlegel, G. E. Scuseria, M. A. Robb, J. R. Cheeseman, V. G. Zakrzewski, J. A. Montgomery, R. E. Stratmann, Jr., J. C. Burant, S. Dapprich, J. M. Millam, A. D. Daniels, K. N. Kudin, M. C. Strain, O. Farkas, J. Tomasi, V. Barone, M. Cossi, R. Cammi, B. Mennucci, C. Pomelli, C. Adamo, S. Clifford, J. Ochterski, G. A. Petersson, P. Y. Ayala, Q. Cui, K. Morokuma, D. K. Malick, A. D. Rabuck, K. Raghavachari, J. B. Foresman, J. Cioslowski, J. V. Ortiz, B. B. Stefanov, G. Liu, A. Liashenko, P. Piskorz, I. Komaromi, R. Gomperts, R. L. Martin, D. J. Fox, T. Keith, M. A. Al-Laham, C. Y. Peng, A. Nanayakkara, C. Gonzalez, M. Challacombe, P. M. W. Gill, B. Johnson, W. Chen, M. W. Wong, J. L. Andres, C. Gonzalez, M. Head-Gordon, E. S. Replogle, J. A. Pople, *Gaussian 98*, Revision A.6, Gaussian, Inc., Pittsburgh PA, **1998**.
[18] a) A. D. Becke, *Phys. Rev. A* **1988**, *38*, 3098–3100; b) C. Lee, W. Yang, R. G. Parr, *Phys. Rev. B* **1988**, *37*, 785–789; c) A. D. Becke, *J. Chem. Phys.* **1993**, *98*, 5648–5652.
[19] W. J. Hehre, L. Radom, J. A. Pople, P. v. R. Schleyer, *Ab initio Molecular Orbital Theory*, John Wiley & Sons Inc., New York, **1986**.
[20] H. B. Schlegel, *J. Comput. Chem.* **1982**, *3*, 214–218.
[21] a) J. Tomasi, M. Persico, *Chem. Rev.* **1994**, *94*, 2027–2094; b) V. Barone, M. Cossi, J. Tomasi, *J. Chem. Phys.* **1997**, *107*, 3210–3221.
[22] L. Onsager, *J. Am. Chem. Soc.* **1936**, *58*, 1486–1493.
[23] D. A. Singleton, Y. Wang, H. W. Yang, D. Romo, *Angew. Chem. Int. Ed.* **2002**, *41*, 1572–1575.
[24] a) C. Gonzalez, H. B. Schlegel, *J. Chem. Phys.* **1989**, *90*, 2154–2161; b) C. Gonzalez, H. B. Schlegel, *J. Phys. Chem.* **1990**, *94*, 5523–5527.

Received: December 23, 2004

